Modelling of a liquid-liquid-solid-gas system: Hydrogenation of dispersed liquid sodium to sodium hydride

Salmi, Tapio; Russo, Vincenzo

Published in:
Chemical Engineering Journal

DOI:
10.1016/j.cej.2018.09.073

Publicerad: 01/01/2019

Document Version
(Referentgranskad version om publikationen är vetenskaplig)

Modelling of a liquid-liquid-solid-gas system: Hydrogenation of dispersed liquid sodium to sodium hydride

Tapio Salmi*, Vincenzo Russo

Åbo Akademi, PCC/Chemical Engineering, Laboratory of Industrial Chemistry and Reaction Engineering, FI-20500 Turku/Åbo, Finland

Università di Napoli 'Federico II', Chemical Science Department, IT-80126 Napoli, Italy

* Corresponding author: tapio.salmi@abo.fi, tel. +358 2 2154427, fax. +358 2 2154479

ABSTRACT

Sodium hydride is a powerful reduction agent used in chemical industry. Industrial production of sodium hydride through hydrogenation of melt sodium dispersed in mineral oil is very demanding because of the complex multiphase system (liquid-liquid-gas-solid) and safety aspects. A new mathematical model was developed for the production of solid sodium hydride from dispersed liquid-phase sodium and molecular hydrogen. New rate equations were derived for the hydrogenation process of dispersed sodium droplets in a semi-batch reactor. The model comprises surface reactions as well as liquid-solid mass transfer effects of hydrogen. The properties of the differential-algebraic model were investigated by numerical simulations and the

model was verified with experimental data of sodium hydrogenation in an isothermal, intensively agitated semi-batch reactor. The kinetic and mass transfer parameters included in the model were estimated successfully with non-linear regression analysis and the model gave a good reproduction of the experimental data. The molecular-level model can be used for the design and optimisation of sodium hydride production processes.

Keywords: sodium hydride, dispersed sodium, hydrogenation, kinetics, mass transfer, semi-batch reactor, mathematical modelling

1 INTRODUCTION

Sodium hydride (NaH) is a strong reducing agent and the raw material of sodium borohydride (tetrahydroborate, $NaBH_4$), which has large applications in chemical and process industries, for instance, in the reduction processes involved in the production of pharmaceuticals and bleaching agents [1-2]. Sodium borohydride is kinetically stable in alkaline aqueous solutions [3], whereas sodium hydride reacts spontaneously and vigorously with water releasing hydrogen and heat [1-2]. Sodium hydride is used as such in for many reactions in organic synthesis, such as alkylation, acylation and Claisen condensation [1]. Sodium hydride is stable up 300^{o}C, at which starts to decompose [1].

Early attempts to make sodium hydride directly via hydrogenation of melt sodium were not very successful, because the solid sodium hydride formed remained dispersed with sodium and inhibited the hydrogenation process. Later on, attempts were made to spread melt sodium and surface-active components on a porous support, which resulted in an improved yield of sodium hydride, but did not lead to a true breakthrough. The method was developed at DuPont and was published by Hansley [4]. Dispersion of sodium in an inert liquid, in which hydrogen is soluble, was the decisive innovation for an efficient industrial production of sodium hydride. The American company Metal Hydrides Inc patented and started the production with the dispersion method in 1957 [5-6], evidently based on the early ideas of Muckenfuss [7]. Nowadays sodium hydride is produced industrially through hydrogenation of metallic sodium (Na(l)) in liquid state. Melt sodium is dispersed in a mineral oil and molecular hydrogen is bubbled through the liquid dispersion. Solid NaH is formed as the reaction product. The reaction can be successfully

conducted at 250-300^{o}C at atmospheric or higher hydrogen pressures. Continuous operation is enabled by using stirred tank reactors coupled in series.

The reaction stoichiometry is given below,

$$Na(l) + (1/2)H_2\,(g) \rightarrow NaH(s)$$

Even though the overall reaction is very well-known [1-2], the detailed surface reaction mechanism between liquid Na and dissolved H_2 has not been thoroughly investigated and analysed hitherto.

In the present work, a hypothesis for the surface reaction mechanism is presented and the corresponding rate equation will be derived. The rate expression is coupled to the mass balances of sodium and sodium hydride. The reaction is presumed to proceed in a semi-batch reactor, where the mineral oil and dispersed sodium co-exist in batch, but gaseous hydrogen is continuously bubbled through the liquid phase. The isothermal reactor is assumed to operate at atmospheric pressure. Experimental data from literature are used to validate the new model for the reaction kinetics and the mass transfer of hydrogen.

2 REACTION MECHANISM AND RATE EQUATIONS

The reaction between Na(l) and H_2 is of topochemical nature, proceeding on the outer surfaces of the dispersed Na droplets. H_2 is assumed to adsorb and dissociate on the Na(l) surface, after which it reacts with a surface atom of Na forming NaH which is released from the surface. The

process is thus very analogical with a catalytic Eley-Rideal mechanism, but in this case, the material of the reactive surface (Na(l)) is consumed during the reaction. Based on these hypotheses, the reaction mechanism can be written as follows,

Reaction step	Stoichiometric number of the step	
$H_2 + 2* = 2H*$	½	(1)
$H* = NaH*$	1	(2)
$NaH* = NaH + *$	1	(3)

where H* denotes adsorbed hydrogen on a sodium atom and NaH* is the key intermediate, reduced hydrogen, i.e. adsorbed sodium hydride. De facto * denotes a sodium atom on the surface, i.e. * =Na*, but the notation * is used for the sake of brevity.

The hydrogen adsorption step is assumed to be rapid, so that the quasi-equilibrium hypothesis can be applied, whereas the quasi-stationary state hypothesis is applied to the sodium hydride (NaH*) on the surfaces of the dispersed sodium droplets. The quasi-equilibrium hypothesis implies for step (1)

$$K_H = \frac{c_H{}^{*2}}{c_H c^{*2}} \tag{4}$$

where K_H and c_H denote the adsorption equilibrium constant and the concentration of dissolved H_2 in the mineral oil. The concentration of adsorbed hydrogen is solved from eq. (4),

$$c_H{}^* = (K_H c_H)^{1/2} c^* \tag{5}$$

The application of the quasi-stationary state hypothesis on NaH* implies for the surface intermediate NaH* that its generation rate is zero,

$$r_{NaH*} = r_2 - r_3 = 0 \quad (6)$$

For the rate of the overall reaction (r) is valid:

$$r = r_2 = r_3 \quad (7)$$

The rates of the elementary steps (2) and (3) can be conveniently expressed as

$$r_2 = k_2 c_H * - k_{-2} c_{NaH} * \quad (8)$$

$$r_3 = k_3 c_{NaH} * - k_{-3} c_{NaH} c * \quad (9)$$

Eqs (8) and (9) are set equal according to eq. (6), and the expression of c_H*, eq. (5), is inserted. The concentration of NaH* can now be expressed with the aid of the concentration of the sodium sites on the droplet surface (c*),

$$c_{NaH*} = \left[\frac{k_2 (K_H c_H)^{1/2} + k_{-3} c_{NaH}}{k_{-2} + k_3} \right] c * \quad (10)$$

The total balance for the sites on the sodium surface is

$$c * + c_H * + c_{NaH} * = c_0 \quad (11)$$

where c_0 denotes the total concentration of surface sites (in mol/m^2).

The expressions (5) and (6) are inserted in eq. (11) after which the concentration of available surface sites of sodium is solved explicitly:

$$c* = \frac{c_0}{1 + \sqrt{} + [\ ]} \quad (12)$$

where $\sqrt{}=(K_H c_H)^{1/2}$ and [ ] denotes the expression in the bracket of eq. (10). After this, the surface concentrations c_{H*} and c_{NaH*} are obtained in a straightforward way:

$$c_H^* = \frac{\sqrt{\ } c_0}{1 + \sqrt{\ } + [\ ]} \tag{13}$$

$$c_{NaH}^* = \frac{[\ ] c_0}{1 + \sqrt{\ } + [\ ]} \tag{14}$$

The overall rate expression is now obtained by inserting eqs (13) and (14) in eq. (8), and recalling eq. (7),

$$r = \frac{(k_2 \sqrt{\ } - k_{-2}[\ ]) c_0}{1 + \sqrt{\ } + [\ ]} \tag{15}$$

A further simplification of eq. (15) is possible, because it is confirmed that solid NaH does not react back to Na(l), which means that k_{-3} becomes negligible.

The content in the bracket [ ] expression is thus compressed to

$$[\ ] = \left[\frac{k_2 (K_H c_H)^{1/2}}{k_{-2} + k_3} \right] \tag{16}$$

The rate equation (15) becomes

$$r = \left(k_2 (K_H c_H)^{1/2} - \frac{k_{-2} k_2 (K_H c_H)^{1/2}}{k_{-2} + k_3} \right) c_0 D'^{-1} \tag{17}$$

where $D' = 1 + \sqrt{\ } + [\ ]$. Under isothermal conditions, the parameters of the model can be merged to a certain degree. We denote

$$k' = \frac{k_2 k_3 K_H^{1/2} c_0}{k_{-2} + k_3} \tag{18}$$

$$K' = \left(1 + \frac{k_2}{k_{-2} + k_3} \right) K_H^{1/2} \tag{19}$$

The rate equation can now be given in a very compressed form, including two adjustable parameters (k' and K') only:

$$r = \frac{k' c_H^{1/2}}{1 + K' c_H^{1/2}} \tag{20}$$

In case that experimental data at different temperatures are available, a deeper analysis of the temperature dependencies of the rate and adsorption parameters becomes possible.

3 MASS BALANCE FOR LIQUID SODIUM

The primary mass balance for Na(l) in the tank reactor can be written as (Na=N)

$$\frac{dn_N}{dt} = r_N A \tag{21}$$

where A is the total outer surface area of melt sodium droplets (Na(l)). The reaction stoichiometry implies that

$$r_N = \nu_N r \tag{22}$$

where ν_N=-1 and r is obtained from eq. (20).

If a monodisperse mixture is presumed, the total surface is directly related to the number of sodium droplets (n_P), $A=n_P A_P$, where A_P is the surface area of an individual droplet. For a perfect spherical droplet, $A_P=4\pi R^2$, where R is the radius of the droplet. The droplet radius is calculated from

$$R = \left(\frac{3Mn_N}{4\pi n_P \rho} \right)^{1/3} \tag{23}$$

after applying elementary physical considerations. The number of droplets (n_P) can however be related to the initial stage with all the droplets having the initial radius (R_0), which implies ($n_P=n_{0P}$):

$$\frac{R}{R_0} = \left(\frac{n_N}{n_{0N}} \right)^{1/3} \tag{24}$$

The total number of droplets is obtained from

$$n_P = \left(\frac{3M}{4\pi\rho R_0{}^3} \right) n_{0N} \tag{25}$$

Combination of eqs (22)-(25) and inserting them in the balance equation (21) gives finally

$$\frac{dn_N}{dt} = \nu_N r \left(\frac{3M}{\rho R_0} \right) n_{0N}{}^{1/3} n_N{}^{2/3} \tag{26}$$

which is valid for perfectly spherical droplets. Non-ideal geometry of a droplet can be taken into account by introducing a shape factor (s) defined by $s+1=(A_P/V_P)R_0$, where R_0 is the characteristic dimension of the droplet. For instance, for spheres is $A_P/V_P=3/R_0$ valid and for infinitely long cylinders $A_P/V_P=2/R_0$. Thus $s+1$ is 3 and 2 for these cases, respectively. Droplets which deviate from ideal spheres have some additional outer surface area, i.e. $s+1>3$. Equation (26) can thus be generalized to

$$\frac{dn_N}{dt} = \nu_N r \left(\frac{(s+1)M}{\rho R_0} \right) n_{0N}{}^{1/(s+1)} n_N{}^{s/(s+1)} \tag{27}$$

After introducing the dimensionless amount of substance, $y=n_N/n_{0N}$, eq. (27) is transformed to

$$\frac{dy}{dt} = \nu_N r \left(\frac{(s+1)M}{\rho R_0} \right) y^{s/(s+1)} \tag{28}$$

for which the following initial condition is valid: y=1 at t=0.

4 MASS BALANCE FOR DISSOLVED HYDROGEN

For hydrogen, a simplified treatment of the mass balances in gas and liquid phases is applied. Hydrogen is continuously bubbled into the dispersion through the stirred tank reactor. Therefore it is reasonable to assume that the concentration of dissolved hydrogen in the bulk phase of the mineral oil is constant and at a saturation state. However, the mass transfer resistance of dissolved hydrogen might play a role in the liquid films surrounding the sodium droplets, depending on the stirring effect used. A local mass balance for the liquid film around the sodium droplets can be expressed as follows,

$$N_H A + \nu_H r A = 0 \tag{29}$$

Eq. (29) assumes a local steady state at the film-droplet interface. A simple expression for the hydrogen flux through the liquid film is based on the law of Fick,

$$N_H = k_{LH}(c_{LH} - c_H) \tag{30}$$

where k_{LH} is the mass transfer coefficient of hydrogen and c_{LH} and c_H denote the hydrogen concentrations in the bulk liquid and on the surface of the droplet. After inserting eqs (20) and (30) in the mass balance (29), we obtain

$$k_{LH}(c_{LH} - c_H) + \frac{\nu_H k' {c_H}^{1/2}}{1 + K' {c_H}^{1/2}} = 0 \tag{31}$$

from which the real concentration (c_H) on the droplet surface is calculated during the solution of the balance equation (28) for sodium. It is practical to bring eq. (31) to a dimensionless form by introducing the variable $x^2=c_H/c_{LH}$, $x<1$. By defining two dimensionless parameters,

$$\alpha = \frac{-\nu_H k'}{k_{LH} c_{LH}^{1/2}} \tag{32}$$

and

$$\beta = K' c_{LH}^{1/2} \tag{33}$$

Eq. (31) is transformed to

$$1 - x^2 - \frac{\alpha x}{1+\beta x} = 0 \tag{34}$$

which is de facto a third-degree equation with respect to x. Parameter α is a measure for the mass transfer resistance. For very vigorous stirring, $k_{LH}\to\infty$, $\alpha\to 0$ and $x\to 1$, i.e. the hydrogen concentration on the droplet surface equals to that in the bulk liquid.

There is however an interesting complication in this treatment. The value of the mass transfer coefficient (k_{LH}) and parameter α are not constant during the course of the reaction even though the stirring rate is kept constant. The reason is that the sodium droplets diminish in size because sodium is consumed in the reaction. The classical correlation for the mass transfer coefficient relates the Sherwood number (*Sh*) to the Reynolds (*Re*) and Schmidt (*Sc*) numbers (Wakao 1984) [8],

$$Sh = a' + b' \mathrm{Re}^{\alpha'} Sc^{\beta'} \tag{35}$$

where

$$Sh = k_{LH} d / D_H \tag{36}$$

and

$$Sc = \upsilon / D_H \tag{37}$$

The droplet diameter (d) is related to the radius: d=2R. The other symbols are defined in Notation.

For stirred tank reactors, the following definition, based on the theory of Kolmogoroff, is proposed,

$$\mathrm{Re} = \left(\frac{\varepsilon d^4}{\upsilon^3} \right)^{1/3} \tag{38}$$

where ε is the energy dissipated to the system via stirring. For the parameters a' and b' (eq. 35) the values a'=2 and b'=1 are generally accepted. The values α'=1/2 and β'=1/3 have been proposed by Temkin (1977) [9]. The numerical value of the mass transfer coefficient (k_{LH}) is obtained from

$$k_{LH} = \frac{D_H Sh}{2R} = \frac{D_H}{2R} (2 + \mathrm{Re}^{1/2}\, Sc^{1/3}) \tag{39}$$

where

$$\mathrm{Re}^{1/2} = \varepsilon^{1/6} (2R)^{2/3} \nu^{-1/2} \tag{40}$$

For silent conditions, Re=0 and k_{LH}=D_H/R, i.e. the film thickness (δ=D_H/k_{LH}) equals the droplet radius. For vigorous stirring, on the other hand, $\mathrm{Re}^{1/2}\mathrm{Sc}^{1/3}$>>2 and eq. (39) is simplified to

$$k_{LH} = \frac{\varepsilon^{1/6} D_H^{\,2/3}}{\upsilon^{1/6} (2R)^{1/3}} \tag{41}$$

Recalling the ratio between the droplet radius (R) and the amount of sodium, eq. (24), and inserting it in eq. (41) gives for the mass transfer coefficient

$$k_{LH} = \frac{\varepsilon^{1/6} D_H^{\,2/3}}{\upsilon^{1/6} (2R_0)^{1/3} (n_N / n_{N0})^{1/9}} \tag{42}$$

Eq. (42) reveals that the mass transfer coefficient increases as the reagent (Na) is consumed because n_N/n_{0N} decreases from 1 towards zero during the course of the reaction.

The dimensionless parameter α (eq. 32) is strongly influenced by the mass transfer coefficient, k_{LH} (eq 42). After taking into account the dependence of k_{LH} on the amount of sodium (n_N), it is rewritten to

$$\alpha = \kappa (n_N / n_{N0})^{1/9} \tag{43}$$

where

$$\kappa = \frac{-\nu_H k' \upsilon^{1/6} (2R_0)^{1/3}}{c_{LH}^{\,1/2} \varepsilon^{1/6} D_H^{\,2/3}} \tag{44}$$

and $n_N/n_{0N}=y$.

Eq. (34) becomes

$$1 - x^2 - \frac{\kappa y^{1/9} x}{1 + \beta x} = 0 \tag{45}$$

and $c_H/c_{LH}=x^2$.

5 SUMMARY OF THE MODEL

The final model used in the simulations and parameter estimations is summarized in Table 1. It is de facto a differential-algebraic model, which is solved numerically by the software gPROMS [10]. A stiff ODE-solver was used for the differential equation, and the algebraic equation was solved iteratively during the course of the main solution. Some special cases can be solved in a simplified way: if the mass transfer is very efficient, x=1 and algebraic equation can be omitted, and if the adsorption of hydrogen on the Na droplets is weak, β=0 and the algebraic equation can be solved analytically as a second-degree equation.

Table 1 Summary of the model

$$1 - x^2 - \frac{\kappa y^{1/9} x}{1 + \beta x} = 0$$

$$\frac{dy}{dDa} = -\frac{x}{1 + \beta x} y^{s/(s+1)} \qquad y=1 \text{ at } Da=0$$

$y=n_N/n_{0N}$, $x=(c_H/c_{LH})^{1/2}$, c_H= the real concentration of H_2 on the Na surface, c_{LH}=the saturation concentration of hydrogen in the mineral oil) and Da=Damköhler number, $Da=[k' c_{LH}^{1/2}(s+1)M/(\rho R_0)]t$. Dimensionless model parameters: β = merged rate-adsorption parameter for hydrogen, κ=mass transfer parameter for hydrogen

---

6 SIMULATION RESULTS AND DISCUSSION

Several numerical simulations were performed by investigating the parameter space and related effects on the evolution of the dimensionless concentration of sodium (y) along Da. The summary of the numerical values used for each simulation is reported in Table 2.

Table 2 – Summary of the parameter used to perform the parametric activity.

Simulation	***β***	***s***	***κ***
1	0	2	0.1
2	0	3	0.1
3	0	4	0.1
4	0	5	0.1
5	0	2	1.0
6	0	2	2.5
7	0	2	5.0
8	1	2	0.1
9	2	2	0.1
10	3	2	0.1
11	4	2	0.1
12	5	2	0.1

The shape factor effect on the reaction is shown in Figure 1-A in the semi-logarithmic plot. The greater difference can be appreciated at high conversion. The κ parameter, related with the liquid-solid mass transfer limitation, has a high influence on the reaction rate. Increasing its value

corresponds to increase the mass transfer limitation, thus a lower hydrogen concentration on the droplet surface is observed (Figure 1-D), leading to a lower reaction rate (Figure 1-B). Finally, the β value increase shows a high deactivating effect on the reaction rate (Figure 1-C).

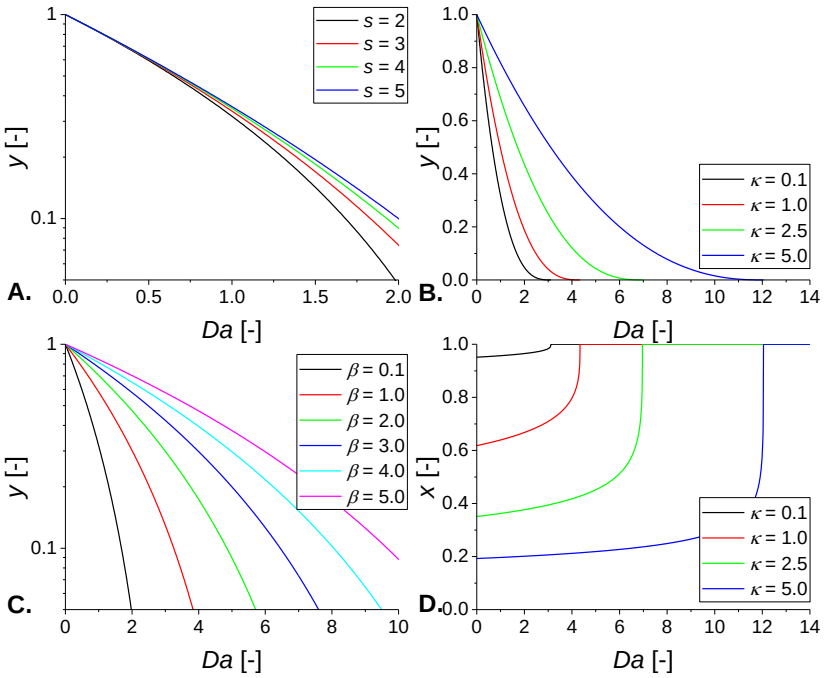

Figure 1. Dimensionless sodium concentration profiles as a faction of *Da* by investigating the effect of the following parameters: A: $s \in$[2-5], B. $\kappa \in$[0.1-5], C. $\beta \in$[0.1-5]. D. x profiles for $\kappa \in$[0.1-5].

7 EXPERIMENTAL DATA AND PARAMETER ESTIMATION

The experimental data for the model verification were obtained from Sjöberg [11]. The kinetic hydrogenation experiments were conducted in an isothermal steel reactor (400 mL), which was operated in semibatch mode. The total mass of sodium and oil was typically 120 g, and the mass ratio of sodium-to-oil was 1:3 (30g:90g). The experimental matrix is summarized in Table 3. Sodium was dispersed in a mineral oil (Risella 15, Shell) after which a flow of hydrogen was switched on. The reactor was operated under atmospheric pressure. An efficient stainless steel rotor-stator disperser (Tornado ET20) was coupled to the reactor. The speed of the disperser was varied between 3000 and 14000 rpm. The hydrogenation temperature was 235-290^{o}C (508-538K). Samples were withdrawn with a vacuum pump from the dispersion during the progress of the reaction. The sodium content of the samples was determined by titration with butyl bromide. Liquid ammonia was used as solvent in the titrations [11]. The total Na and NaH contents of some samples were analysed by titration with HCl. The mass balance was closed: NaH was the only product detected and at complete conversion, all the sodium metal had been converted to sodium hydride. The droplet size was monitored by taking microscopic images from the samples. The diminishing of the droplet size due to the reaction was confirmed and no accumulation of solid sodium hydride layer on the droplets could be seen. The hydrogen flow out from the reactor vessel was monitored visually. The hydrogen flow was always in large excess compared to the hydrogenation rate.

Table 3. Summary of the experimental conditions adopted for each experiment.

EXP	***T* [K]**	***v* [rpm]**	$\dot{V}_{H2}$ **[m^3/s]**
1	508	10000	$5.0 \cdot 10^{-6}$
2	523	10000	$5.0 \cdot 10^{-6}$
3	538	10000	$5.0 \cdot 10^{-6}$
4	538	10000	$16.7 \cdot 10^{-6}$
5	538	3000	$5.0 \cdot 10^{-6}$
6	523	7000	$5.0 \cdot 10^{-6}$
7	523	14000	$5.0 \cdot 10^{-6}$

A summary of experimental results is provided in Figures 4-6. Some qualitative conclusions can be drawn. The reaction proceeds already at 230ºC, even though the reaction time for a complete conversion would become very high. At 250ºC the rate is rather high, and a complete conversion is attainable. The dispersion starts to be unstable as 260ºC is exceeded (sodium droplets start to coalesce), and thus these data cannot be modelled together with data obtained at lower temperatures (Figure 2). An increase of the rotation speed of the disperser increases the reaction rate, as illustrated by Figure 3. This is at least partially due to the effect of the stirring speed on the droplet size. At 10000 rpm the droplet diameter was around 25 μm, but at 5000 rpm it was around 70 μm. An increase of the hydrogen flow improves slightly the hydrogenation rate, but the effect is rather modest, as displayed in Figure 4.

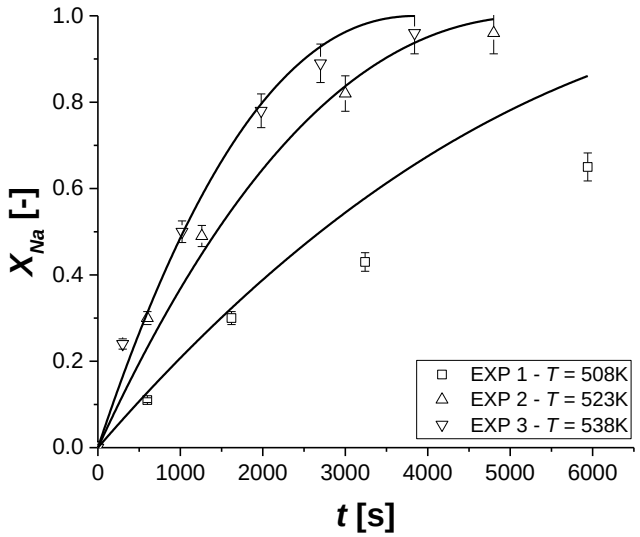

Figure 2. Sodium conversion profiles for experiments performed at different temperatures. Continuous lines represent model predictions.

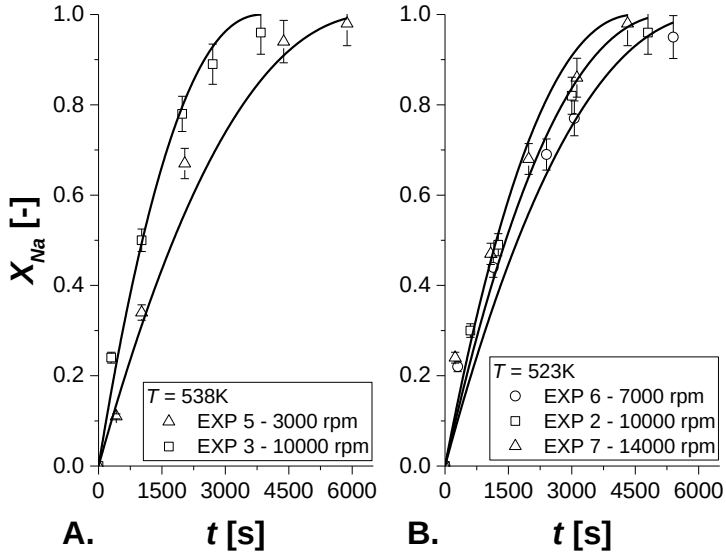

Figure 3. Effect of the stirring rate on the sodium conversion at: A. 538K; B. 523K. Continuous lines represent model predictions.

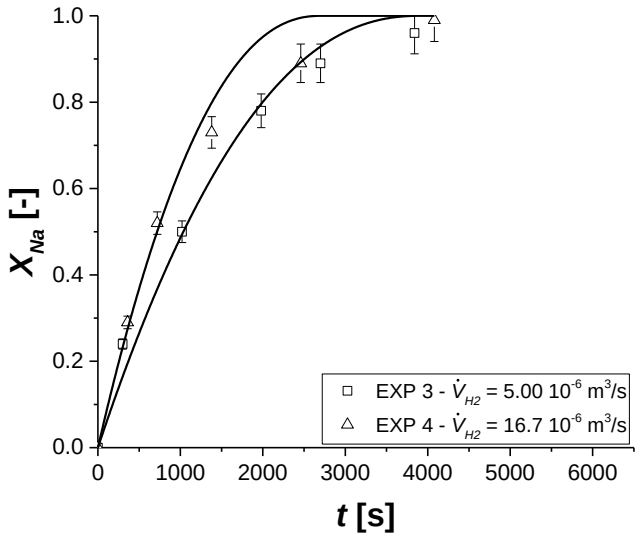

Figure 4. Effect of the hydrogen flow-rate on the sodium conversion profiles. Continuous lines represent model predictions.

The parameter estimation was commenced with a simplified approach. Data obtained at different temperatures, disperser speeds and hydrogen flows were treated separately. It is presumed that the mineral oil is saturated with respect to hydrogen during the reaction because hydrogen is continuously fed into the liquid phase. Consequently, the first part of the right-hand side of eq. (27) is constant during an isothermal experiment. A dimensionless quantity $y=n_N/n_{0N}$ is introduced and the constant part is merged to a parameter (a). The differential equation (28) becomes

$$\frac{dy}{dt} = -ay^{s/(s+1)} \tag{46}$$

where

$$a = |\nu_N| r\left(\frac{(s+1)M}{\rho R_0}\right) \tag{47}$$

Separation of variables and integration with the limits y=1 and y gives

$$1 - y^{1/(s+1)} = \frac{at}{s+1} \tag{48}$$

For complete conversion of sodium y=0 and the corresponding time for complete reaction is denoted by τ. After inserting this condition in eq. (48) we obtain $a/(s+1)=1/\tau$. Eq. (48) can now be compressed to

$$1 - y^{1/(s+1)} = t/\tau \tag{49}$$

The conversion of sodium is X=1-y. Now eq. (49) becomes

$$F = 1 - (1 - X)^{1/(s+1)} = t/\tau \tag{50}$$

By assuming a value for the shape factor (s), plots of the function F vs time (t) can be prepared. A linear plot indicates the validity of the shrinking particle model. A set of plots is provided in Figure 5, demonstrating the linear trend predicted by the model (s=2). The degree of explanation exceeded 90% in these plots.

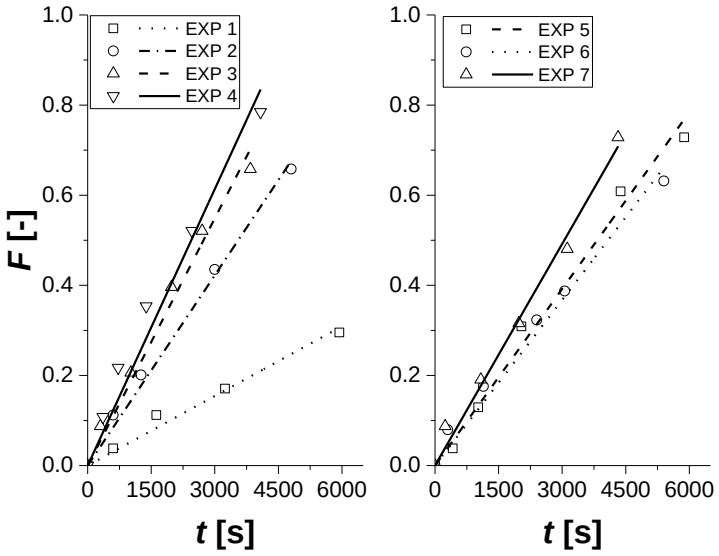

Figure 5. *F* function (eq. 50) plot vs the reaction time for each experiment. Calculated values were obtained by linear fit on the experimental data.

For the sake comparison, the corresponding linear plot $F(X)$ vs t for the product layer model [12] was prepared. The plots became somewhat bended, and the degree of explanation was about 80%, i.e. clearly less than for the shrinking particle model.

The final parameter estimation was carried out by applying non-linear regression directly on the experimental data displayed in Figures 2-4. Based on the proposed mechanism and the related mathematical treatment, the following forms of the mass balance equations were used:

$$\frac{dy}{dt} = -\frac{k''' x}{1+\beta x} y^{s/s+1} \tag{51}$$

$$1 - x^2 - \frac{\kappa y^{1/9} x}{1+\beta x} = 0 \tag{52}$$

where y is the dimensionless sodium concentration, while $x^2=c_H/c_{LH}$, the ratio of the real hydrogen concentration on the droplet surface to the bulk concentration. The merged rate parameter is $k'''= k' c_{\mathrm{LH}}^{1/2}(s+1)M/(\rho R_0)$. The following initial condition was presumed: $y=1$ at $t=0$.

The dependency of parameter κ on the stirring rate (v) was simplified as described by Equation 53, assuming that the dissipated energy is proportional to the stirring rate at a power of 3 [13]. Parameters β and k''' were assumed to have Arrhenius and van't Hoff like temperature dependencies as shown below, imposing T_{ref}=538K,

$$\kappa = \frac{-\nu_H k' \upsilon^{1/6} (2R_0)^{1/3}}{c_{LH}^{1/2} \varepsilon^{1/6} D_H^{2/3}} = \frac{-\nu_H k' \upsilon^{1/6} (2R_0)^{1/3}}{c_{LH}^{1/2} (\kappa_1 \nu^{1/2}) D_H^{2/3}} = \kappa_0 \nu^{-1/2} \tag{53}$$

$$k''' = k'''_{ref}\left[\frac{-E_a}{R_G}\left(1/T - 1/T_{ref}\right)\right] \tag{54}$$

$$\beta = \beta_{ref}\left[\frac{-\Delta H}{R_G}\left(1/T - 1/T_{ref}\right)\right] \tag{55}$$

The numerical values of the parameters, along with the confidence intervals, are listed in Table 4. As revealed by the table, the accuracies of the parameters are good.

The fit of the model to the experimental data can be checked by looking at Figures 4-6. From the parity plot reported in Figure 6, it is evident that the agreement between the experimental data and the predictions is good and the model is sufficient for the description of the experimental data. The experiments performed at at 538K were simulated by assuming that the emulsion at high temperature is unstable. The instability implies that the initial radii of the droplets are larger at 538K than at 508K and 523K. Equation (28) reveals the effect of the initial radius (R_0) of the droplet on the reaction rate: doubling of the initial radius decreases the rate by 50%. This might be due to the instability of the dispersion, which becomes more evident with increasing temperatures. As a result of the parameter estimation, the reference kinetic constant at 538K is roughly 0.8 times the one at lower temperatures.

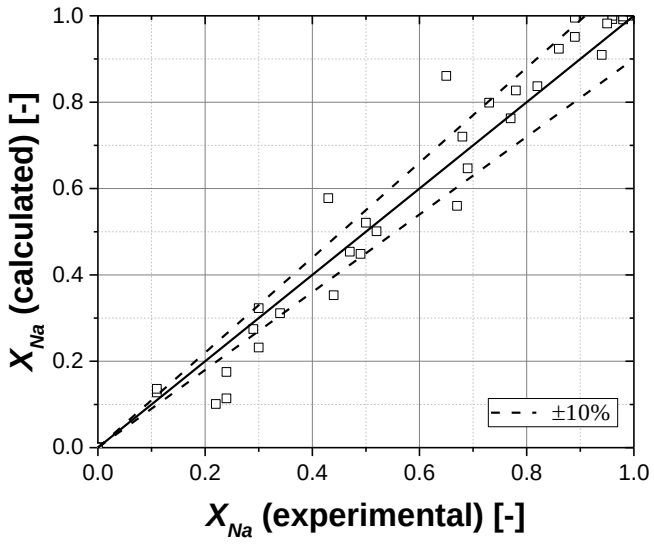

Figure 6. Parity plot for NaH formation kinetics. Dashed lines correspod to ±10% window error.

The effect of the hydrogen flow rate on the conversion was described by fitting k'''_{ref} separately on the experiment conducted with the hydrogen flow rate of $1.67 \cdot 10^{-5} m^3/s$, as the parameter merges also the bulk hydrogen concentration that depends on the feed flow rate. As revealed by the numerical values reported in Table 2, the kinetic constant is 1.1 times larger. Thus, the effect on the hydrogen flow rate on the sodium conversion was relatively small. The model predictions are displayed in Figure 4. For much lower hydrogen flow rates, the effect might become even more visible, because the interfacial gas-liquid mass transfer starts to influence the overall rate. This was confirmed in few preliminary experiments with lower hydrogen flow rates, before selecting the standard hydrogen flow rate.

The correlation for the mass transfer coefficient was applied to describe the experimental data by merging the constant part in the adjustable parameter (κ, eqs 43 and 44). Implementation of this

correlation was implemented gave satisfactory results in describing the collected experimental data.

Table 2 – Parameter estimation activity results with related statistics. The confidence intervals (CI) are calculated at 95%. *Value calculated for T=538K. **Value calculated for hydrogen flow-rate of $1.67 \cdot 10^{-5} m^3/s$.

Parameter	***Value***	***95% CI***	***Unit***
k'''_{ref}	$4.46 \cdot 10^{14}$	$\pm 0.34 \cdot 10^{14}$	s^{-1}
$k'''_{ref}{}^{*}$	$3.65 \cdot 10^{14}$	$\pm 0.15 \cdot 10^{14}$	s^{-1}
$k'''_{ref}{}^{**}$	$4.93 \cdot 10^{14}$	$\pm 0.24 \cdot 10^{14}$	s^{-1}
E_a	$92.76 \cdot 10^{3}$	$\pm 5.92 \cdot 10^{3}$	J/mol
β_{ref}	5.92	± 0.57	-
ΔH	$65.36 \cdot 10^{3}$	$\pm 5.35 \cdot 10^{3}$	J/mol
κ_0	$5.93 \cdot 10^{19}$	$\pm 0.68 \cdot 10^{19}$	$(rpm)^{-1/2}$

8 CONCLUSIONS

Industrial production of sodium hydride is a very demanding process because it requires simultaneous treatment of melt sodium and molecular hydrogen at elevated temperatures. The feasible technology is based on the hydrogenation of finely dispersed sodium droplets in mineral oil. In this way, the process can be operated in a safe way and high yields of solid sodium hydride are obtainable. For successful process design and optimisation, a reliable kinetic and mass transfer model is necessary. An advanced mathematical model, based on plausible reaction mechanisms on the surface of melt sodium and interfacial mass transfer of hydrogen was developed. Numerical simulations of the model, a differential-algebraic system, were conducted and the model was verified with experimental hydrogenation data obtained from an isothermal semi-batch reactor.

NOTATION

A	surface area, m^2
a	merged parameter in eq. (46)
a', b'	coefficients in the correlation for Sherwood number, eq. (35) -
c	concentration, mol/m^3
c^*	concentration on the sodium surface, mol/m^2
c_0	total concentration of sites on the sodium surface, mol/m^2
D	diffusion coefficient, m^2/s
D'	denominator of eq. (17), -
d	droplet diameter (=2R), m
E_a	activation energy, J/mol
F	test function in eq. (50), -
ΔH	enthalpy, J/mol
K	adsorption equilibrium constant, m^3/mol
K'	merged parameter, eq. (19), -
k	reaction rate constant
k'	merged rate constant, eq. (18), $mol/(m^2 s)/(mol/m^3)^{1/2}$
k'''	merged rate constant, eq. (51), s^{-1}
k_L	mass transfer coefficient, m/s
M	molar mass, kg/mol
N	diffusion flux, $mol/(m^2 \cdot s)$
n	amount of substance, mol
n_P	number of droplets in the liquid phase

R droplet radius, m

R_G gas constant, 8.3143 J/(Kmol)

r rate, mol/(m^2·s)

s shape factor, -

T temperature

t time, s

X conversion of sodium

x dimensionless hydrogen concentration, -

y dimensionless amount of sodium, -

Greek letters

α, β dimensionless parameters, eqs (32)-(33), -

α', β' exponent in the correlation (35) for Sherwood number -

δ film thickness, m

ε dissipated energy, W/kg

κ dimensionless parameter, -

ν stoichiometric coefficient, -

υ kinematic viscosity, m^2/s

ρ density, kg/m^3

τ reaction time for complete conversion, s

Dimensionless numbers

Da Damköhler number, -

Re Reynolds number, -

Sc Schmidt number, -

Sh Sherwood number, -

Subscripts and superscripts

H	hydrogen
L	mass transfer or solubility in liquid phase
P	droplet
ref	reference
*	surface site
0	initial state

ACKNOWLEDGEMENT

This work is a part of activities at the Johan Gadolin Process Chemistry Centre (PCC), a centre of excellence in scientific research financed by Åbo Akademi University.

REFERENCES

[1] Kirk-Othmer Encyclopedia of Chemical Technology, 4th Ed., Vol 13, 606-629, Wiley, New York, 1995

[2] Ullmann's Encyclopedia of Industrial Chemistry, 6th Ed., Vol 16, 721-7226, Wiley-VCH Weinheim, New York, 2003

[3] M.M. Kreevoy, R.W., Jacobson, The rate of decomposition of $NaBH_4$ in basic aqueous solutions, Ventron Alembic 15 (1979) 2-3

[4] V.L. Hansley, P.M. Charlisle, The Production of Sodium Hydride and Some of its Reactions, Chemical Engineering News 23 (1945) 1332-1380

[5] M.D. Banus, R.W. Bragdon, Method for preparing borohydrides of alkali metals, US Patent 2,720,444 (1955)

[6] S.W. Fedor, M.D. Banus, D.P. Ingalls, Potassium borohydride manufacture, Ind. Eng. Chem. 49 (1957) 1664-1672

[7] A.M. Muckenfuss, Process for the manufacture of alkali metal hydride, US Patent 1,958,012 (1934)

[8] N. Wakao, Recent Analysis of Chemically Reacting Systems (Ed. Doraiswamy, L.K.), Wiley Eastern, New Delhi, 1984

[9] M.I. Temkin, Transfer of dissolved matter between a turbulently moving liquid and particles suspended in it, Kinetika i Kataliz 18 (1977) 493-496

[10] gPROMS Model Builder, Process Systems Enterprise (https://www.psenterprise.com/) (last visited 11/06/2018)

[11] Sjöberg, B., Reaktionsteknisk undersökning av en slurryreaktor, Master's thesis, Åbo Akademi Turku/Åbo Finland (1980)

[12] T. Salmi, J.-P. Mikkola, J. Wärnå, Chemical Reaction Engineering and Reactor Technology, CRC Press Taylor & Francis Group, Boca Raton Fl., 2011

[13] K. Bimlesh, Energy Dissipation and Shear Rate with Geometry of Baffked Surface Aerator, Chemical Engineering Research Bulletin 14 (2010) 92-96